POLISH ACADEMY OF SCIENCES - MATERIALS SCIENCE COMMITTEE
SILESIAN UNIVERSITY OF TECHNOLOGY OF GLIWICE
INSTITUTE OF ENGINEERING MATERIALS AND BIOMATERIALS
ASSOCIATION OF ALUMNI OF SILESIAN UNIVERSITY OF TECHNOLOGY

Conference Proceedings

11th INTERNATIONAL SCIENTIFIC CONFERENCE
ACHIEVEMENTS IN MECHANICAL & MATERIALS ENGINEERING

Microstructure and tensile behaviour of cold-rolled TRIP-aided steels

A. Wasilkowska[a], P. Tsipouridis[a], E.A. Werner[a], A. Pichler[b], S. Traint[b]

[a]Christian-Doppler-Laboratorium für Moderne Mehrphasenstähle, Lehrstuhl für Werkstoffkunde und Werkstoffmechanik, Technische Universität München, Germany

[b] Voestalpine Stahl, Linz, Austria

The transformation of austenite to martensite is fundamental to the hardening of carbon steels. This transformation plays an important role for the mechanical behaviour of low-carbon ferrous alloys containing about 10 vol.% retained austenite. The effect, known as transformation induced plasticity, is manifested by unusual high work hardening and high uniform elongation - properties very desirable for thin sheets applied for automobiles parts. Tensile tests of cold-rolled sheets at room temperature allowed to study the retained austenite stability against strain induced martensitic transformation. The influence of the processing texture (specimen orientation) and the strain rate ($2{\cdot}10^{-2}$, $2{\cdot}10^{-3}$ s^{-1}) on the uniform elongation were observed experimentally. Results show that a homogeneous microstructure and the absence of initial blocky martensite ensure a long deformation paths. At the same time, tensile data reveal only a small influence of deformation parameters on the ultimate strength.

1. INTRODUCTION

The development of lightweight and high strength automobile parts led to the specification of high-strength low-carbon steels for automotive applications [1]. It is well recognized that due to transformation induced plasticity (TRIP), low-carbon TRIP-aided steels exhibit advantageous mechanical properties compared to single-phase cold-formable steels. Good welding and galvanizing quality are additional factors leading to the enhanced demand of such materials [2].

The chemical composition of conventional TRIP-steels is in the range of Fe, 0.15-0.4 C, 1-2 Mn and 1-2 Si (mass content in %). Their microstructure consists of ferrite, bainite and some retained austenite, with a typical grain size of a few micrometers. The stability of retained austenite against strain induced martensitic transformation (SIMT) is a major factor governing the plasticity of the material. This effect can be described as follows [3]: (i) At a critical tensile stress, retained austenite transforms irreversibly to martensite in strain-concentration areas. (ii) SIMT is accompanied by a volume expansion of the transforming region, which leads to additional plastic accommodation and work hardening of the surrounding microstructure. (iii) This results in a delay of macroscopic necking and ultimately leads to higher uniform and total elongations.

Investigations on processing technology show that alloying with aluminium, copper, phosphorus or niobium have a beneficial effect on retarding austenite decomposition and on mechanical properties [4-6]. Martensite growth at low strains hinders plastic formability due to an insufficient uniform elongation, on the other hand, too stable austenite is detrimental to the ultimate strength. The present studies concentrate on microstructure and room-temperature tensile properties of currently produced TRIP-aided steels.

2. EXPERIMENTAL PROCEDURE

TRIP 700 steels are produced at voestalpine Stahl Linz. The cold-rolled sheets have a thickness of 1.2 mm, their chemical composition is: Fe–0.2 wt. %C – 1.5-1.7 wt. %(Si+Al) – 1.5 wt.% Mn. Two charges were investigated - one with 0.6 wt.%Si (high-Si variant) and a second one with 0.4 wt. %Si (low-Si variant).

A two-step heat treatment was performed in a continuous annealing simulator. In the first step, the material is annealed at 800°C in the $\alpha+\gamma$ region. There, cementite dissolves and the relative amounts of ferrite and austenite are adjusted, simultaneously to recrystallization of the cold-rolled material. After intercritical annealing, the material is slowly cooled to 700-650^{o}C and then rapidly cooled to the bainitic range. Bainitic transformation parameters were 400^{o}C/400s for the low-Si variant and at T= 300, 350, 400^{o}C for t= 60, 120, 240, 480 s for the high-Si variant.

Room-temperature tensile tests were performed according to the standard EN 10002. The high-Si variant specimens were prepared parallel to the cold-rolling direction and pulled to different strain levels at a strain rate of $4\cdot10^{-3}$ s^{-1}. The low-Si variant specimens were prepared according to DIN 50114 for thin-sheet materials. Specimens were cut at different inclinations to the rolling direction of the sheet and deformed at a strain rate of of $2\cdot10^{-2}$ and $2\cdot10^{-3}$ s^{-1} up to fracture. Reference marks on the gauge length make possible to calculate the true stress and true strain within each length section.

Thermodynamical calculations with the program ThermoCalc were performed to study the influence of the alloying elements on the Fe-C-Mn-Si-Al system. Phase structure was revealed by light microscopy (LM) applying two-step etching procedure with V2A and Klemm's etchants [7]. Thin foils were prepared for transmision electron microscopy (TEM) using double-jet polishing in a Struers A-8 electrolyte. To study the transformation behaviour of retained austenite during straining, the content of retained austenite was measured as a function of strain by a magnetic volumetric method [8].

3. RESULTS AND DISCUSSION

Fig. 1 shows the calculated concentration section (Fe-C) of the Fe-C-Mn-Si-Al system. The carbon content of the investigated alloys is indicated by a vertical line. ThermoCalc predictions using the steel databases TCFE and SSOL showed, that after annealing at 800^{o}C the austenite fraction is about 45 vol. % and its carbon concentration is about 0.5 wt. %C. The same values were obtained from both databases.

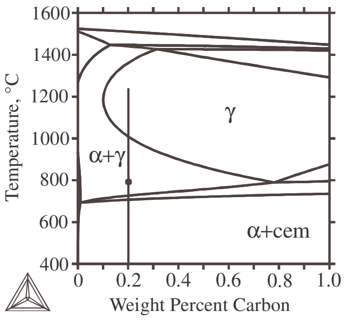

Fig. 1. Calculated concentration section (Fe-C) of the Fe-C-Mn-Si-Al system.

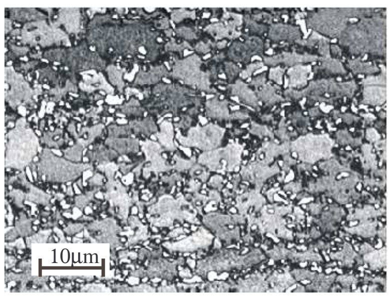

Fig. 2. LM image of high-Si variant steel transformed at 400°C for 480 s; austenite - white, ferrite - grey, bainite - dark.

3.1. Microstructure characterization

Fig. 2 shows a typical microstructure of as-isothermally transformed steels. Retained austenite (RA) particles exhibit a mean size of 0.8 μm. Metallographic investigations show that RA is mainly located at the ferrite grain boundaries and is frequently surrounded by bainite. A significant influence of the chemical composition and the heat treatment on the location and morphology of the retained austenite could not be detected. The maximum content of retained austenite was about 14 vol. % when employing temperatures of 300-400°C and times between 60-120s. The amount of RA in isothermally transformed steel is much less than could be expected from the equilibrium concentration section shown in Figure 1.

a) b)

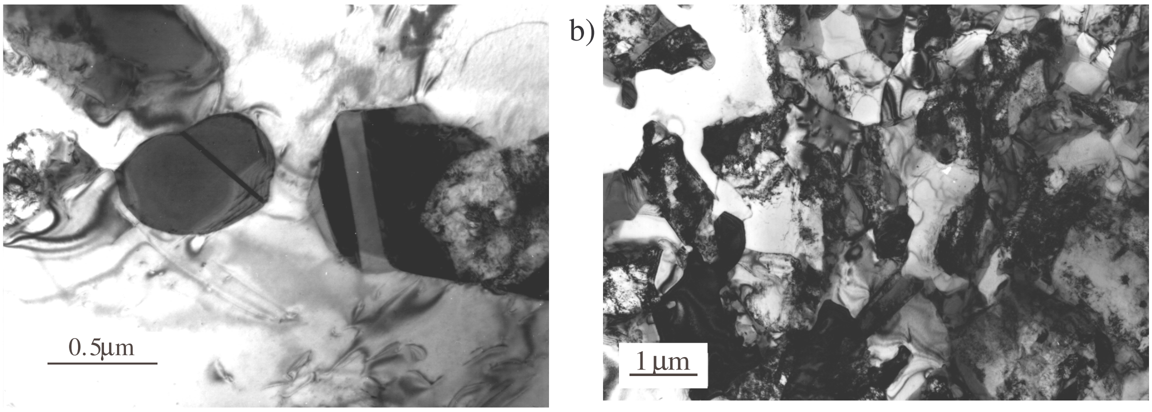

Fig. 3. TEM images of low-Si variant steel transformed at 400°C/400 s; a few isolated RA grains /dark/ in a ferritic matrix (a) and an overview of the neighbouring phases (b).

Fig. 3 shows the microstructure as obtained by TEM. The single austenite grains detected in dark contrast on the image (Fig. 3a) show preferred crystallographic orientation to ferrite, which is close to the Kurdjumov-Sachs relationship. The ferrite grain structure is characterized by a nonequiaxed morphology (Fig. 2) and may contribute to the strength by both smaller grain size and increased dislocation density compare to a polygonal morphology [9]. The bainite structure is quite difficult to describe due to the complexity of the transformation reaction. The "classical bainite" morphology is characterized by ferrite laths of high dislocation density ($0.5 - 5\times10^{11}$ cm^{-2}) and includes carbide precipitates [10]. In TRIP-aided steels a similar morphology is observed, however, without carbide formation (Fig. 3b). The carbon supersaturated in the "bainitic ferrite" is partitioned into the residual austenite soon after the diffusion-less transformation [11].

3.2. Room-temperature mechanical properties

TRIP-steels show high work hardening, which may be attributed to the formation of martensite and the accumulation of dislocations in the soft ferritic matrix. The strain hardening coefficient *n* as a function of true strain is defined as [12]:

$$n = \frac{d(\ln\sigma)}{d(\ln\varepsilon)} \tag{1}$$

Fig. 4 shows the influence of the bainitic transformation temperature after 240s of annealing time on the n-values. The diagram clearly shows an increase of work hardening with increasing strain for the material annealed at 400°C. Decreasing n-values for steels annealed at 300 and 325°C are an indication of the vanishing TRIP-effect at high plastic strains.

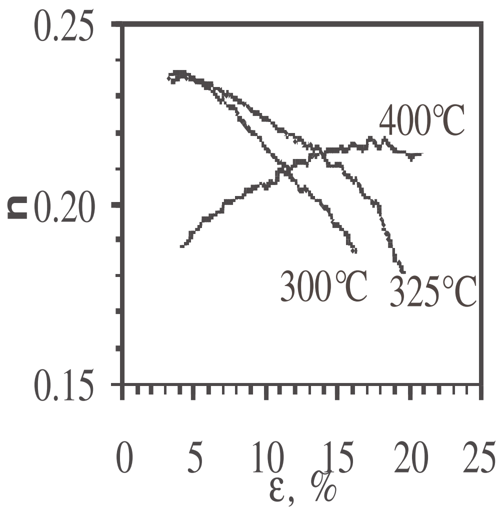

Fig. 4. Dependence of strain hardening coefficient *n* on the true strain ε after different annealing treatments.

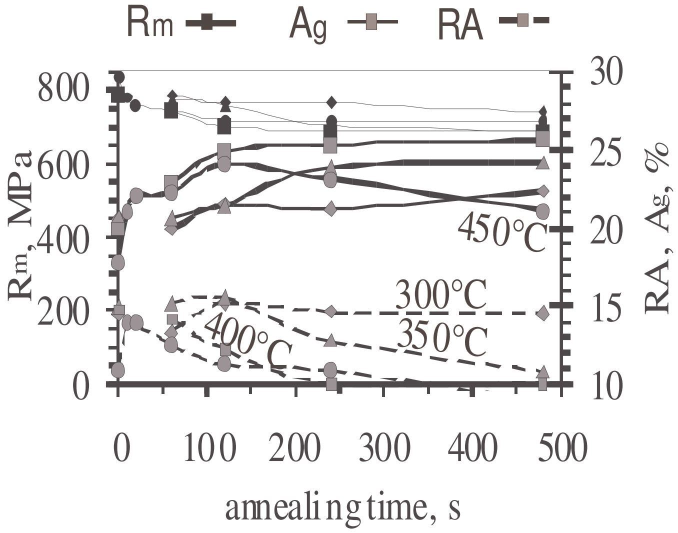

Fig. 5. Room-temperature strength R_m and uniform elongation A_g of the high-Si variant, and amount of retained austenite RA, as a function of annealing parameters.

Fig. 5 is a summary of mechanical behaviour for the materials annealed between 300 and 450°C, presented together with the content of retained austenite in the as-transformed TRIP-aided steels. The best combination of strength and uniform elongation, $R_m \times A_g$ =17500 MPa·%, was obtained for a bainitic temperature of 400°C and an annealing time of 120-480s, which is related to a sufficient stability of retained austenite against strain induced martensitic transformation.

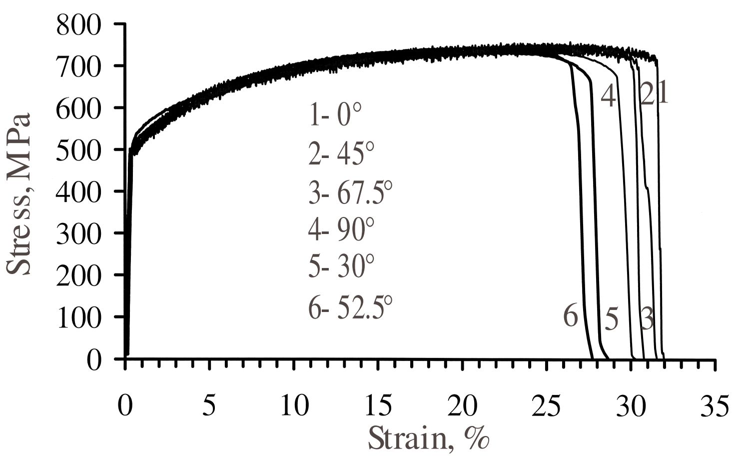

Fig. 6. Room-temperature stress-strain curves of the low-Si variant steel. The angle between the tensile axis and the sheet rolling direction is marked for the strain rates $2{\cdot}10^{-2}$ (5, 6) and $2{\cdot}10^{-3}$ s^{-1} (1-4).

The low-Si variant is characterised by 700 MPa as ultimate tensile strength and a uniform elongation of above 25 %. The results of tensile tests show (Fig. 6), that the relative orientation of the tensile axis to the cold-rolling direction of the sheet influences the total and uniform elongation at room temperature. Increasing the angle from 0^o to 90^o decreases the total elongation from 32% to 30%, respectively, at a strain rate $2{\cdot}10^{-3}\ s^{-1}$. At the higher strain rate, the uniform elongation is between A_g= 27-30%. At the same time, the tensile data in Fig. 6 reveal only a small texture dependence of the ultimate tensile strength.

3.3. Transformation of retained austenite upon straining

A set of curves relating the fraction of transformed austenite particles to the true tensile strain is shown in Fig. 7 for the high-Si variant.

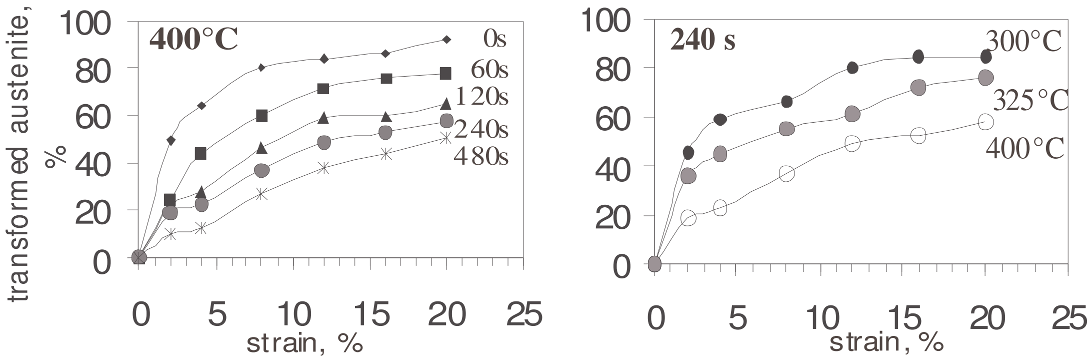

Fig. 7. Fraction of transformed austenite particles as a function of true strain for the high-Si variant. Dependence on annealing time (a) and on annealing temperature (b).

The results show that either no bainitic treatment at all or annealing at 300°C lead to an almost complete austenite to martensite transformation upon straining, whereas sufficient long anneals at 400°C are beneficial for increasing austenite stability up to large plastic strains.

4. FURTHER COMMENTS

Tensile tests on two TRIP-aided steels show the orientation and strain rate dependence of their mechanical behavior. The optimum stability of retained austenite is achieved by proper heat treatment of cold-rolled materials.

Attempts to find out the correlations between processing parameters, chemical composition, microstructure and mechanical properties of TRIP-aided steels have to deal with the high complexity of the microstructure (variability of morphology, size and composition). The structural phases surrounding retained austenite can decisively contribute to its stability against SIMP by their crystallographic relationship to austenite grains and their in-situ yield strength governed e.g. by solid solution hardening. Moreover, the macroscopic flow stress should be described by implementing the strain and stress dependent phase transformation kinetics.

According to some strengthening models, replacing dispersed austenite by a harder constituent introduces geometrically necessary dislocations in the surrounding ferrite in order to accommodate the volume expansion and lattice shear. The martensite microstructure and morphology depend mainly on the transformation mechanism, which should be investigated further. The total transformation strain due to SIMT depends on the number of martensite variants activated, whose selection is strongly dependent on the loading conditions, i.e. the direction of the load with respect to the crystallographic orientation of the transforming RA grain [13]. This may be one of the reasons for the texture dependence of transformation kinetics observed experimentally. The models developed recently based on evolution algorithms take into account the local stresses in multiphase systems as a function of the deformation temperature [14]. Introduction of a “tensorial thermodynamic flux” into the macroscopic material law of TRIP-steels might be a further step allowing to distinguish between the movement of phase boundaries and the deformation of the body [15].

REFERENCES

1. Proc. ISIJ: ULSAB Advance vehicle concepts, Technical transfer dispatch #6, May 2001, Brussels, Belgium, 2001.
2. Proc. Int. Conf. on TRIP-aided High Strength Ferrous Alloys, 19-21. June 2002, Ghent University, B. C. De Cooman (ed.), GRIPS, Bad Harzburg, 2002.
3. T. Yokoi, K. Kawasaki, M. Takahashi, K. Koyoma and M. Mizui, Tech Notes/JSAE Review, 17 (1996) 210.
4. S. Traint, E. A. Werner, A. Pichler and P. Stiaszny, BHM, 144 (1999) 362.
5. S. Traint, A. Pichler, P. Stiaszny and E.A.Werner, Proc. 44th Mechanical Working and Steel Processing Conference, 8th Int. Rolling Conference and International Symposium on Zinc-Coated Steels, Vol. XL, September 8-11, 2002, Orlando, Florida, Iron & Steel Society 2002, p. 139.
6. W. Bleck, K. Hulka and K. Papamantellos, Mat. Science Forum A284-286 (1998) 327.
7. G. Perzow, Metallographisches, keramographisches, plasto-graphisches Ätzen, Gebrüder Bornträger, Berlin-Stuttgart, 1994.
8. E. Wirthl, A. Pichler, R. Angerer, P. Stiaszny, K. Hauzenberger, Y. F. Titovets and M. Hackl, Proc. Int. Conf. on TRIP-aided High Strength Ferrous Alloys, 19-21. June 2002, Ghent, B.C. De Cooman (ed.), GRIPS, Bad Harzburg, 2002, p. 61.
9. H. K. D. H. Bhadeshia, Bainite in steels, The Institute of Materials, London, 1992.
10. Atlas of Bainitic Microstructures: Continuous cooled microstructures of low-carbon steels, vol. 1, Iron and Steel Institute of Japan, Tokyo, 1992, p. 4.
11. E. Girault, P. Jacques, P. Ratchev, J. Van Humbeeck, B. Verlinden and E. Aernould, Mater. Sci. Eng. A273-275, (1999) 471.
12. J. B. Austin and R. L. Rickett, Trans. Amer. Inst. Min. Met. Eng. 135 (1939) 386.
13. G. Reisner, F.D. Fischer, Y. H. Wen and E.A. Werner, Metall. Mater. Trans., 30A (1999) 2583.
14. H. Vogelsang, Parameteridentifikation für ein selbst-konsistentes Stoffmodell unter Berücksichtigung von Phasentransformationen, Mitteilungen aus dem Institut für Mechanik, nr 129, Ruhr-Universität Bochum, Germany, 2001.
15. C. Oberste-Brandenburg and O. T. Bruhns, A tensorial description of the transformation kinetics of the martensitic phase transformation, Int. Journal of Plasticity, submitted